

# A Review study on the Comparative Study on Wind Load (Along & Across) Analysis of Reinforced Concrete Chimney by (i) Gust factor method (ii) Simplified Method & (iii) Random Response Method

<sup>1</sup>Shivam Kumar, <sup>2</sup>Ankush Kumar Jain

<sup>1</sup>M.Tech Student, <sup>2</sup>Assistant Professor, Civil Engineering Department  
Poornima University, Jaipur, India

\*\*\*

**Abstract** - This research will be conducted to determine the Comparative Study on Wind Load (Along & Across) Analysis of Reinforced Concrete Chimney by (i) Gust factor method (ii) Simplified Method & (iii) Random Response Method of a Reinforced Concrete chimney. This thesis deals with external applied loadings that effect chimney structures namely along and across wind load, with reference to the IS875 (Part-III) IS4998(Part-I) & Draft code CED38(7892):2013. The compressive strength of cement concrete is assuming M35 grade in severe condition, tensile strength of steel 550D TMT, wind zone is VI. For Zone VI wind speed is 55m/s. Modelling and Analysis will be done in Staad V8i software. Analytical results will be compared to achieve differences in results of the structures against the wind forces.

**Key Words:** Steel Structure, Load, wind screen, chimney

## 1. INTRODUCTION

A chimney is a building that encloses the flue and works with it to create a system that vents hot gases or smoke into the open air. Chimneys are normally vertical or almost vertical to ensure a smooth flow of gases and to attract air into the combustion, commonly known as the stack effect or chimney effect. The majority of industrial chimneys built today, including those in Turkey, around the world, use reinforced concrete (RC). Due to outdated construction methods or inadequate seismic design, chimneys built in the late 1970s and earlier may be susceptible to damage during earthquakes. Compared to current codes, earlier ones do not provide enough seismic details.

### 1.1 Effects of Load on Chimneys

Different kinds of loads are applied to RC concrete chimneys in both lateral and vertical directions. Aside from the structure's own weight and the pressures placed on the service platforms, the main loads that a concrete chimney typically encounters are pressure from wind loads, loads brought on by seismic activity, and temperature loads. Since concrete chimneys are often relatively tall and slender constructions, the impacts of wind on RC chimneys have a significant impact on their structural behaviour.

### 1.2 Along Wind Load

The drag component of the wind force pushing on the chimney wall causes along wind load effects. The wind speed, the wind's surface contact area, the form, and the orientation of the structure all affect how much pressure the wind exerts on its surface. The structure is modelled as a cantilever structure with a fixed base to evaluate the impact of wind on the chimney. The pressure brought on by the wind load in this model is acting perpendicular to the exposed surface of the RC chimney. For the purpose of evaluating along wind loads, the structure is modeled as a bluff body.

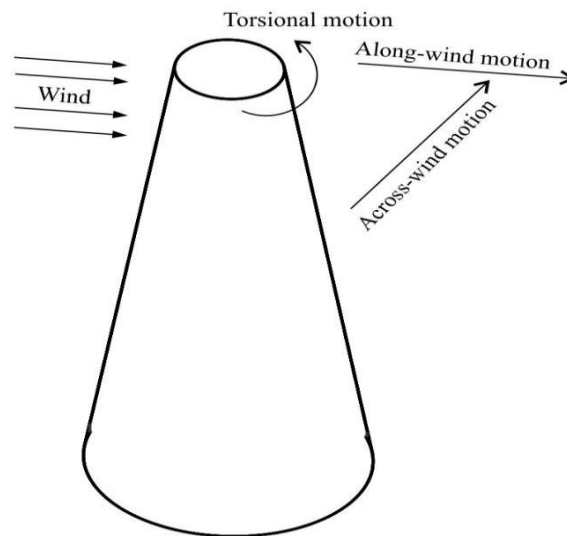


Fig. 1.1 wind effects with respect to its direction of flow

### 1.3 Wind Force Analytical Method

- (a) Gust Factor Method
- (b) Simplified Method
- (c) Random Response Method

## 2. LITERATURE REVIEW

### Arzpeyma et al., (2020)

The usage of solar energy in the modern period is required and important as well. Solar chimney technology for power generation is one of the solar energy harvesting systems where the direct and diffused solar radiations are absorbed in the solar chimney power plant. The usefulness of solar chimneys has been established for power generation, and it is a viable solution to future energy generation plans. This article presents a thorough description of the study and development of solar energy technology as well as the history of solar chimneys in the last few decades.

### Zuo,et al., (2020)

This research proposes the wind supercharged solar chimney power plant (WS-SCPP) model by putting an unpowered wind pressure wheel at the top of the chimney. Solar chimney power plant (SCPP) prototype in Spain is used as the basis for building physical and mathematical models of WS-SCPP and comparing its performance to that of the SCPP. By using an unpowered wind pressure wheel, WS-performance SCPP's significantly improves. The shaft power of WS-SCPP is always greater than that of SCPP at the same turbine rotational speed. At 100 rpm, the shaft power of SCPP increases from 37.8kw to 57.03kw by 50.9 percent.

### Zuo,et al., (2020)

Solar chimney power plants combined with seawater desalination and waste heat (WSCPPDW) and solar chimney power plants combined with seawater desalination and waste heat (SCPPDW) have been proposed in this article. The key difference between the two was the existence or lack of a wind supercharging system, both of which had a spiral exhaust gas heating channel (SGC). The output qualities were then evaluated under various scenarios using physical and mathematical models that were built. WSCPPDW and SCPPDW both performed better when the chimney height and flue gas temperature were both increased. All output qualities improved when seawater thickness was reduced. Flue gas flow and sun irradiation both rose at the same time, but freshwater output and overall efficiency decreased as a result.

**Shi, L. (2019)**

Wind and solar chimney interactions were studied computationally and conceptually. It's the wind angle ( $\theta$ ), the angle formed by the outward normal of the wall and the wind direction, that determines whether or not a higher wind speed corresponds to better performance. The scenario with  $\theta = 0$  has the best performance in a windward situation ( $0^\circ$  to  $90^\circ$ ). Even though the leeward situation with  $\theta = 180^\circ$  has a little favourable effect, the scenarios with  $90^\circ$  to  $180^\circ$  have negative effects, which is somewhat surprising. When  $\theta$  is  $0^\circ$  or  $45^\circ$ , the area of the window ( $A_w$ ) has a beneficial impact on airflow, with a linear relationship between  $A_w 0.34$  and  $A_w 0.46$ . Predicting airflow rates under  $90^\circ$  was made possible using a theoretical model, which may be used to make similar forecasts for  $90^\circ$  to  $180^\circ$ . There is a good correlation between the forecasts and the numerical data.

**Zuo, et al.,(2020)**

WSCPPDW (wind supercharging solar chimney power plant with seawater desalination and gas waste heat) was investigated in this study. For this article, the main goal is to investigate the impact of operational and structural aspects on the WSCPPDW's performance and to analyse its flow field characteristics. Structure parameters and flue gas jet could not be well captured by a previous WSCPPDW mathematical model. As a result, CFD ANSYS Fluent was used to do a 3D numerical simulation of WSCPPDW. Simulations with various turbine rotational speeds, nozzle lengths, chimney outlet radii, and chimney mixing section lengths were run to determine the best operational and structural characteristics for WSCPPDW. Flue gas jets can create a high-temperature, high-speed jet area in the chimney, causing entrainment of the surrounding airflow.

**Górski, P. (2017)**

A tall industrial chimney was subjected to wind excitations to explore its dynamic features, such as its natural frequencies, mode forms, and structural damping ratios, by using GPS technology to monitor horizontal dynamic displacements along its vertical profile. In this case, Frequency Domain Decomposition (FDD) was used to do the study. Based on the results of a static test, the basic properties of GPS background noise are evaluated in the temporal and frequency domains. Three GPS rover units were used to conduct the field testing on the chimney at Belchatow Power Plant in Poland. In order to measure the chimney's horizontal deformation along a vertical profile as a result of the wind, GPS units were mounted on three levels of the chimney.

**Carvalho, et al.,(2019)**

A tall industrial chimney was subjected to wind excitations to explore its dynamic features, such as its natural frequencies, mode forms, and structural damping ratios, by using GPS technology to monitor horizontal dynamic displacements along its vertical profile. In this case, Frequency Domain Decomposition (FDD) was used to do the study. Based on the results of a static test, the basic properties of GPS background noise are evaluated in the temporal and frequency domains. Three GPS rover units were used to conduct the field testing on the chimney at Belchatow Power Plant in Poland.

**3. METHODOLOGY**

The chimney taken into consideration in this study is a commercial reinforced concrete chimney. Wind analysis code were used in the structure's design. For a continuous emission measurement system on the chimney, a door measuring has been proposed to be opened. This chimney was specifically chosen for this investigation in order to assess the impact of such an opening. The chimney has not sustained any damage as a result of the earthquakes.

**3.1 Modeling of Chimney**

STAAD Pro, Bentley software, is used to model the chimney in order to do linear elastic analysis on the structure. A four-node thin shell element is used to simulate a reinforced concrete chimney. The shell element comprises four nodes, and each node has six degrees of freedom, including rotations about the x, y, and z axes as well as translations in the x, y, and z direction.

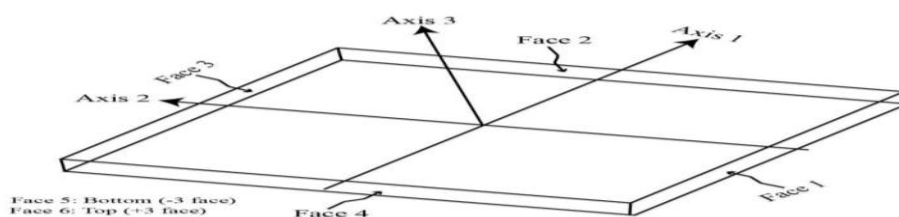


Fig. 3.1 Geometry of thin shell element

Since the chimney's height to diameter ratio is low and its behaviour is that of a thin shell, which does not take into account transverse shear deformation, the chimney is likely to fail flexurally. It depicts the geometry of a thin shell element with four nodes. Four-noded shell elements are used in the chimney's design.

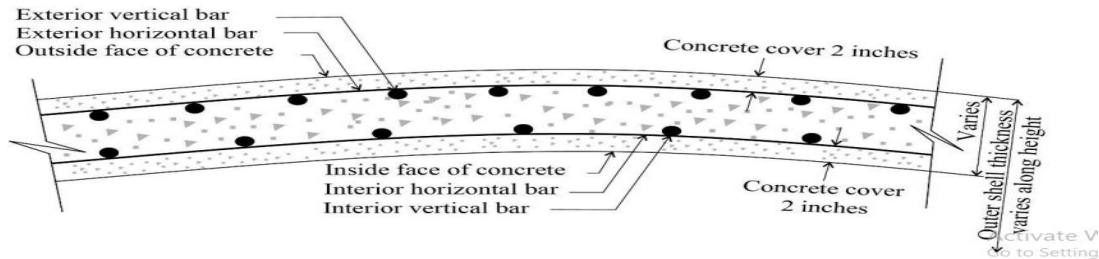


Fig. 3.2 Typical section through column wall of RC chimney

The chimney has a consistent circumferential thickness, but the wall thickness varies along the height of the chimney, leading to varied shell thicknesses, as was previously mentioned in section. It was required to geometrically model the shell elements in a way that avoided the stress concentration in order to produce realistic model results. This was done by making sure that the wall taper is accurately modelled and that the nodes of the shell elements are connected properly.

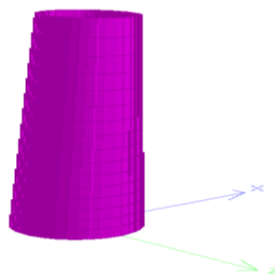


Fig. 3.3 3D view of Chimney

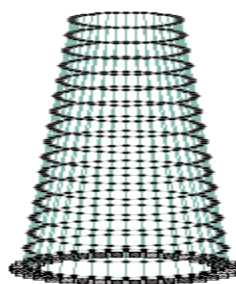


Fig.3.4 Geometrical view of chimney

Mesh density is a crucial metric for accuracy management. Shell elements are discretized to produce correct analysis results by breaking up the bigger elements into a finite number of smaller elements, resulting in a mesh of small area elements. When loading is applied to the area element, it disperses the weight evenly, aiding in the achievement of satisfactory outcomes.

## 4. MODELING AND ANALYSIS

### 4.1 Wind Load Calculation

#### Guest Factor Method

The IS 875 (part 3):1987 states that the basic wind speed can be computed.

$$V_z = V_b * K_1 * K_2 * K_3$$

- $V_z$ = design wind speed at any height  $z$  m/s
- $K_1$ = probability factor (risk coefficient)
- $K_2$ = terrain, height and structure size factor
- $K_3$ = topography factor

### Simplified Method

An air stream on a bluff body, such as a chimney, is obstructed by a static force known as drag force. The form and direction of the wind incidence determine how the wind pressure is distributed. This results in circumferential bending, which is particularly severe for chimneys with larger diameters. Along-wind shear forces and bending moments are also produced by drag force.

### Drag Force

A single stationary bluff body has a drag force of,

$$F_d = \frac{1}{2} C_d \cdot A \cdot \rho_a \cdot \bar{U}^2$$

$F_d$ = drag force, N

$C_d$  = Drag coefficient

$A$  = area of section normal to wind direction, sq. m

The Reynolds number, geometry, and aspect ratio of a structure all influence the drag coefficient value. Re affects the radial distribution of wind pressure on the horizontal segment. Shear forces that are induced in the structure often offset the resultant force of an along wind. On the circumference of the chimney cell, these shear forces are thought to fluctuate sinusoidally.

## 5. CONCLUSION

An industrial chimney is designed and analyzed by three different methods (Gust factor, Simplified method, Random response method). The analytical result is compared on different properties (Pressure, Deflection, Shear Stress and Moment) after review paper.

- The analysis shows that the maximum pressure is obtained at 150 mm height is 19.370 Kn/m<sup>2</sup> by random response method whereas 2.846 Kn/m<sup>2</sup> is obtained via simplified method and least pressure obtained by 2.381 Kn/m<sup>2</sup>. Hence, Gust factor method is more effective than other methods.
- Deflection analysis reported that random response method given height value of deflection that is .705 m and .126 m obtained by simplified method and .1084 m by Gust method. Hence, according to deflection point of view gust factor is more reliable and random response is less reliable.
- Random response method gives highest shear stress that is 870000 N/m<sup>2</sup> through random response method, whereas 240000 N/m<sup>2</sup> and 210000 N/m<sup>2</sup> shear stress value is observed by simplified and gust factor method. Hence, Gust factor is more effective as compare to other method.
- Moment analysis reported that random response method given height value of moment that is 43400 N-m and 6230 N-m obtained by simplified method and 5000 N-m by Gust method. Hence, according to moment point of view gust factor is more reliable and random response is less reliable.

## 6. REFERENCES

- Arzpeyma, M., Mekhilef, S., Newaz, K. M., Horan, B., Seyedmahmoudian, M., Akram, N., & Stojcevski, A. (2020). Solar chimney power plant and its correlation with ambient wind effect. *Journal of Thermal Analysis and Calorimetry*, 141(2), 649-668
- Zuo, L., Qu, N., Liu, Z., Ding, L., Dai, P., Xu, B., & Yuan, Y. (2020). Performance study and economic analysis of wind supercharged solar chimney power plant. *Renewable Energy*, 156, 837-850.
- Zuo, L., Liu, Z., Ding, L., Qu, N., Dai, P., Xu, B., & Yuan, Y. (2020). Performance analysis of a wind supercharging solar chimney power plant combined with thermal plant for power and freshwater generation. *Energy Conversion and Management*, 204, 112282.
- Shi, L. (2019). Impacts of wind on solar chimney performance in a building. *Energy*, 185, 55-67.
- Zuo, L., Dai, P., Liu, Z., Qu, N., Ding, L., Qu, B., & Yuan, Y. (2020). Numerical analysis of wind supercharging solar chimney power plant combined with seawater desalination and gas waste heat. *Energy Conversion and Management*, 223, 113250.
- Elias, S., Matsagar, V., & Datta, T. K. (2017). Distributed multiple tuned mass dampers for wind response control of chimney with flexible foundation. *Procedia engineering*, 199, 1641-1646.
- Wang, Q., Zhang, G., Li, W., & Shi, L. (2020). External wind on the optimum designing parameters of a wall solar chimney in building. *Sustainable Energy Technologies and Assessments*, 42, 100842.
- Méndez, C., & Bicer, Y. (2021). Integrated system based on solar chimney and wind energy for hybrid desalination via reverse osmosis and multi-stage flash with brine recovery. *Sustainable Energy Technologies and Assessments*, 44, 101080.
- Zuo, L., Dai, P., Ding, L., Yan, Z., Wang, X., & Li, J. (2021). Effect of chimney shadow on the performance of wind supercharged solar chimney power plants: A numerical case study for the Spanish prototype. *Global Energy Interconnection*, 4(4), 405-414.
- de Oliveira Neves, L., & da Silva, F. M. (2018). Simulation and measurements of wind interference on a solar chimney performance. *Journal of Wind Engineering and Industrial Aerodynamics*, 179, 135-145.
- Gholamalizadeh, E., & Chung, J. D. (2017). A comparative study of CFD models of a real wind turbine in solar chimney power plants. *Energies*, 10(10), 1674.
- Zuo, L., Liu, Z., Dai, P., Qu, N., Ding, L., Zheng, Y., & Ge, Y. (2021). Economic performance evaluation of the wind supercharging solar chimney power plant combining desalination and waste heat after parameter optimization. *Energy*, 227, 120496.
- Zuo, L., Liu, Z., Qu, N., Dai, P., Sun, Y., & Qu, B. (2020, September). Economic analysis of a wind supercharging solar chimney power plant combined with thermal plant for power and freshwater generation. In *2020 12th IEEE PES Asia-Pacific Power and Energy Engineering Conference (APPEEC)* (pp. 1-6). IEEE.
- Pradhan, S., Chakraborty, R., Mandal, D. K., Barman, A., & Bose, P. (2021). Design and performance analysis of solar chimney power plant (SCPP): A review. *Sustainable Energy Technologies and Assessments*, 47, 101411.
- Zuo, L., Ding, L., Chen, J., Zhou, X., Xu, B., & Liu, Z. (2018). Comprehensive study of wind supercharged solar chimney power plant combined with seawater desalination. *Solar Energy*, 166, 59-70.
- Zuo, L., Liu, Z., Zhou, X., Ding, L., Chen, J., Qu, N., & Yuan, Y. (2019). Preliminary study of wind supercharging solar chimney power plant combined with seawater desalination by indirect condensation freshwater production. *Desalination*, 455, 79-88.
- Khan, M., & Roy, A. K. (2017). CFD simulation of wind effects on industrial RCC chimney. *Int J CivEngTechnol*, 8, 1008-1020.
- Datta, G., Sahoo, A., & Bhattacharjya, S. (2020). Wind fragility analysis of RC chimney with temperature effects by dual response surface method. *Wind and Structures*, 31(1), 59-73.
- Cheng, X., Qian, H., Wang, C., & Fu, X. (2018). Seismic response and safety assessment of an existing concrete chimney under wind load. *Shock and Vibration*, 2018.

- de Oliveira Neves, L., & da Silva, F. M. (2018). Simulation and measurements of wind interference on a solar chimney performance. *Journal of Wind Engineering and Industrial Aerodynamics*, 179, 135-145.
- Kazemi, K., Ebrahimi, M., Lahonian, M., & Babamiri, A. (2022). Micro-scale heat and electricity generation by a hybrid solar collector-chimney, thermoelectric, and wind turbine. *Sustainable Energy Technologies and Assessments*, 53, 102394.
- Setareh, M. (2021). Comprehensive mathematical study on solar chimney powerplant. *Renewable Energy*, 175, 470-485.